# Fast Stress and Rest Acquisitions for Technetium-99m-Sestamibi Separate-Day SPECT

E. Gordon DePuey, Kenneth J. Nichols, Jacek S. Slowikowski, William J. Scarpa Jr., Christopher J. Smith, Steven Melancon and Shawna Newman

*St. Luke's-Roosevelt Hospital and Columbia University College of Physicians and Surgeons, New York, New York*

Abbreviated acquisition protocols were designed for stress and rest to decrease stress and rest SPECT image acquisition times but maintain the high count density of $^{99m}$Tc-sestamibi separate-day cardiac images. **Methods:** Scan findings were compared visually and quantitatively with standard SPECT for 12 rest and 32 stress patient studies. **Results:** Of 29 stress defects detected by standard SPECT, 27 were present with the fast technique; of 8 resting SPECT defects, all were detected with fast SPECT. Two stress and no resting false-positive defects occurred with fast SPECT. Linear correlations (r) between standard and fast quantitative defect extent and severity were 0.76 and 0.86, respectively for stress SPECT, and 0.88 and 0.96 for rest SPECT. Stress fast defects were slightly less severe (p = 0.02) than those observed using standard acquisition. **Conclusion:** We conclude that these fast protocols for separate-day $^{99m}$Tc-MIBI SPECT accurately detect and characterize perfusion defects and provide a means to improve patient tolerance and increase laboratory throughput.

**Key Words:** myocardial perfusion imaging; single-photon emission computed tomography; technetium-99m-sestamibi

**J Nucl Med 1995; 36:569–574**

To obtain high quality diagnostic studies, the image acquisition protocol currently recommended for sestamibi SPECT employs a high-resolution collimator and 25-min imaging times, slightly longer than those routinely used for thallium SPECT (1,2). Capitalizing on the higher dose and photon flux afforded by $^{99m}$Tc-sestamibi, we have developed and evaluated a protocol where image acquisition times are shortened to 8 min for the stress study and 10 min for the rest study, potentially providing better patient tolerance and improved laboratory efficiency.

## METHODS

### Preliminary Phantom Studies

Preliminary work was done using a cardiac phantom (Data Spectrum Corp., Chapel Hill, NC) loaded with 2.5 $\mu$Ci/ml $^{99m}$Tc in the simulated myocardium. Background activity in the simulated phantom's surrounding chest cavity was 1.2% of myocardial activity. This experiment thereby reproduced the imaging parameters encountered in separate-day stress sestamibi imaging as closely as possible.

Two myocardial perfusion defects were created, simulating defects frequently observed in clinical studies. A mid septal 2.2-cm defect contained no activity and had a 100% severity and a distal anterior 4.5-cm defect had a 50% severity.

Using a commercially available single-headed detector system (XCT Camera, General Electric Medical Systems, Milwaukee, WI) and circular 180° orbit (45° right anterior oblique to 45° left posterior oblique), SPECT images with a 6.4 mm slice thickness were obtained using a high-resolution collimator and the standard 25-min acquisition protocol, an 8-min acquisition with the high-resolution collimator, and 25- and 8-min acquisitions with a low-energy, all-purpose (LEAP) collimator (Table 1). The low-energy, all-purpose collimator has a FWHM spatial resolution of 10.2 mm and a sensitivity of 335 counts/min/$\mu$Ci for a source in air at 10 cm from the collimator. In contrast, the high-resolution collimator has a FWHM resolution of 8.1 mm and sensitivity of 195 counts/min/$\mu$Ci at 10 cm.

Image acquisition with the 8-min LEAP protocol yielded a count density 61% of that with the 25-min high-resolution collimator despite only 32% of the imaging time. Phantom SPECT images demonstrating defect contrast and resolution are shown in Figure 1. Thus, for stress we felt the 8-min LEAP protocol afforded the best savings of time and relative preservation of count density.

Contrast was computed from the short-axis slice which best showed the defect as (max − min)/(max + min), where "min" was the lowest count in the simulated myocardium at the defect site, and "max" was the highest count in that same slice. All four of the imaging protocols resulted in similar defect contrast (Table 2). Image contrast of approximately 50% for each method accurately reflected the true 50% contrast of the 4.5-cm defect. However, the true 100% contrast of the small 2.2-cm defect was only 40% for either LEAP protocol, and only slightly better (44%) for either of the two HRP protocols.

For the 8-min acquisition, Butterworth and Hanning filters were evaluated regarding their effects on defect contrast (Table 3

## TABLE 1
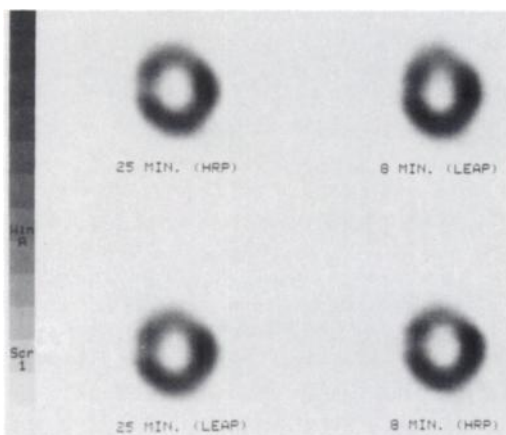### Technetium-99m-Sestamibi Cardiac Phantom Data Acquisitions

| | LEAP collimator | | HRES collimator | |
|---|---|---|---|---|
| | 8 min | 25 min | 8 min | 25 min |
| Energy window | 20% Symm | Same | Same | Same |
| Orbit | 180° Circ | Same | Same | Same |
| No. projections | 32 | 64 | 32 | 64 |
| Time/Projection | 15 sec | 25 sec | 15 sec | 25 sec |
| Total time | 8 min | 25 min | 8 min | 25 min |
| Total counts | 486K | 1,289K | 228K | 796K |

LEAP = low-energy, all-purpose and HRES = high-resolution.

## TABLE 2
### Measured Defect Contrast for Phantom Data Analyzed with a Butterworth 0.45 (Order = 10) Filter

| | 2.2 cm defect | 4.5 cm defect |
|---|---|---|
| | Contrast = 100% | Contrast = 50% |
| 8 min (LEAP) | 40% | 48% |
| 25 min (HRP) | 44% | 52% |
| 8 min (HRP) | 44% | 52% |
| 25 min (LEAP) | 40% | 52% |

and Fig. 2). Contrast of the 4.5-cm 50% defect was equivalent for each of the filters. However, the Butterworth filter with either a 0.45 or 0.55 cutoff frequency and a power of 10 provided the best image contrast of the 100% 2.2-cm defect.

On the basis of both visual and quantitative analysis of these phantom studies, minimizing the acquisition time while increasing count density and defect contrast, the fast acquisition protocol outlined in Table 4 for separate-day stress studies was chosen. For comparison, the standard 25-min protocol is also outlined. In summary, the shorter acquisition time with fast protocol is compensated for by using the LEAP collimator, half the number of stops and a filter with a lower cutoff frequency.

Since the count density in resting sestamibi studies using the separate-day protocol is always somewhat less than that of stress studies (approximately 50%) due to the lack of stress-induced coronary hyperemia, we arbitrarily increased our image acquisition time from 8 min to 10 min for resting separate-day fast studies. This 25% increase in acquisition time is slightly greater than that used for the standard protocol, wherein acquisition time is increased by 20%, from 25 to 30 min. The acquisition and processing parameters we used for resting studies are listed in Table 4 and compared to the standard separate-day resting protocol. The only other parameter for the resting protocol that was different from the fast stress protocol was that the cutoff frequency for the Butterworth filter was further decreased to 0.40 to accommodate potentially lower count density images. Although

no similar alteration in cutoff frequency is used for the standard separate-day sestamibi processing protocol, in our experience resting images seem somewhat count-poor occasionally, so we elected to include this modification.

Thus, in summary, compared to 50 min for the standard protocol, the total acquisition time for the fast protocol we developed is 8 min for the stress study plus 10 min for the resting study, or 18 min, just 36% of the standard protocol's acquisition time.

### Patient Studies

To evaluate the separate-day fast stress imaging protocol, 32 patients selected randomly were imaged first using the standard 25-min protocol and within 30 min thereafter using the 8-min fast protocol. To evaluate the resting fast protocol, 12 other patients were imaged with both the standard 25-min protocol and the 10-min fast protocol. A dose of 22 mCi $^{99m}$Tc-sestamibi was used for all stress and rest studies. Among the 44 total patients studied (19 female and 25 male), body habitus varied. Chest circumferences ranged from 34 to 46 inches. Over 75% of patients had either documented coronary artery disease or a high clinical pretest likelihood. Since the purpose of this study was to compare imaging methods and not to assess test accuracy however, cardiac catheterization was not required for enrollment.

Mean image count density was evaluated for each image acquisition by drawing manual regions of interest (ROIs) around the epicardial limits of the mid left ventricular short-axis tomographic slice.

Studies were interpreted subjectively by three experienced observers unaware of the acquisition protocol. Short-axis, vertical long-axis and horizontal long-axis tomograms, as well as polar plots were viewed. The left ventricle was divided into 12 segments (septal, anterior, lateral and inferior quadrants in the basal, mid



FIGURE 1. Dependence of defect resolution on collimation and acquisition time. LEAP = low-energy, all-purpose; HRP = high-resolution, parallel-hole.

## TABLE 3
### Technetium-99m-Sestamibi Measured Defect Contrast Using Different Filters

| | 2.2-cm defect | 4.5-cm defect |
|---|---|---|
| | Contrast = 100% | Contrast = 100% |
| Butterworth Cutoff = 0.45 Order = 10 | 40% | 48% |
| Butterworth Cutoff = 0.55 Order = 10 | 40% | 48% |
| Hanning Cutoff = 0.70 | 28% | 48% |
| Hanning Cutoff = 0.85 | 32% | 48% |
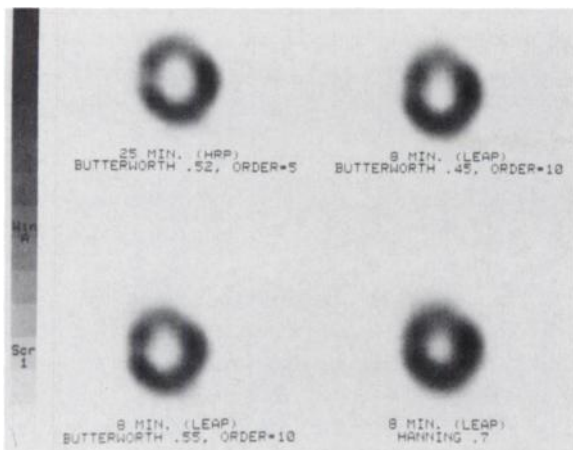
**FIGURE 2.** Dependence of defect resolution on filtering.

and apical thirds of the left ventricle) according to conventional nomenclature and perfusion defects were judged to be present or absent by concensus. Defect severity was also judged to be mild, moderate or marked.

In addition, studies were analyzed quantitatively using commercially available software (Cequal, GE Medical Systems). By comparison to gender-matched normal limits, defect extent (the number of pixels significantly below normal limits) and defect severity (the number of standard deviations below normal limits of those pixels) were determined (3).

## RESULTS

For stress imaging, mean left ventricular (LV) count density measured from mid-ventricular short-axis slices averaged approximately 35% less using the 8-min fast protocol as compared to the 25-min standard protocol (162 ± versus 248 ± 94 counts/pixel). For the resting studies, the LV count density was nearly the same using the 25-min standard protocol and the 10-min fast protocol (225 ± 70 versus 237 ± 67 counts/pixel). Thus, the fast imaging protocols maintained adequate SPECT image count density. All three observers judged all fast data sets to be of adequate technical quality for interpretation.

In the stress images in the 32 patients studied, 29 defects involving a total of 86 myocardial segments were detected visually using the standard protocol. Twenty-seven defects were seen using both the standard and fast protocols. Defect severity (mild, moderate or marked) was judged to be equivalent in all cases except four using either technique. In those four cases, defects appeared one grade less severe using the fast protocol. Two defects were seen only with the standard protocol. Two additional defects were observed with the fast protocol which were not seen using the standard protocol. The source of these two defects is unclear. Although they could be true-positive for coronary disease, coronary angiographic correlation was not available. Although these defects could have been artifactual, no patient motion or attenuation effects could be demonstrated. Agreement between the two methods for defect detection was 87%. With regard to interpretation of a myo-

cardial segment as normal or abnormal, agreement between the two protocols was 98.7%.

In the 12 patients undergoing resting imaging using both protocols, eight defects were detected and were subjectively graded of similar severity. All eight defects were seen with both the standard and fast protocols. Agreement between the two methods with regard to detection of segmental defects was 100%. However, four defects (50%) were judged to be less severe with the fast protocol.

By means of quantitative analysis, defect extent and severity were evaluated using the standard and fast protocols. We recognize that the commercially available software program we used has been documented only for single-day rest/stress sestamibi studies using a predefined acquisition and processing protocol. For the present study, however, we are comparing two different protocols against the same normal patient files and thus, this method should be valid to compare the two protocols used. By linear regression analysis, there was a fairly good correlation between defect extent using the standard protocol (r = 0.76) for stress imaging (Fig. 3). In 4 of 29 defects, extent was smaller using the fast protocol. Similarly, there was a fairly good correlation between the two methods in determining defect severity (r = 0.86) (Fig. 4). Again, in four cases defect severity was less using the fast protocol.

Due to the small number of resting defects (only eight), a similar analysis of resting defects was suboptimal. However, the correlation between the standard and fast protocols for determining the defect extent and severity was fairly good. (r = 0.88 and r = 0.96, respectively) (Figs. 5 and 6). In resting images, as observed with stress studies, both defect extent and severity were underestimated in a minority of cases (2) using the fast protocol.

### Patient One: Normal

For the stress scan in this normal female, corresponding short-axis slices from the apex to the base are displayed for the standard and fast protocols (Fig. 7). Image resolution

**TABLE 4**
Technetium-99m-Sestamibi Standard and Fast Acquisition and Processing Protocols

| | Standard | Stress Fast | Rest Fast |
|---|---|---|---|
| Dose | 22 mCi | same | same |
| Energy window | 20% symmetric | same | same |
| Collimator | HRP | LEAP | LEAP |
| Orbit | 180° circular | same | same |
| No. projections | 64 | 32 | 32 |
| Time/projection | 20 sec | 15 sec | 20 sec |
| Total time | 25 min | 8 min | 10 min |
| Filter | 2-D Butterworth | same | same |
| Cutoff | 0.52 | 0.45 | 0.40 |
| Power | 5 | 10 | 10 |

LEAP = low-energy, all-purpose; and HRES = high resolution.

**Stress Defect Extent by Quantitative Analysis**
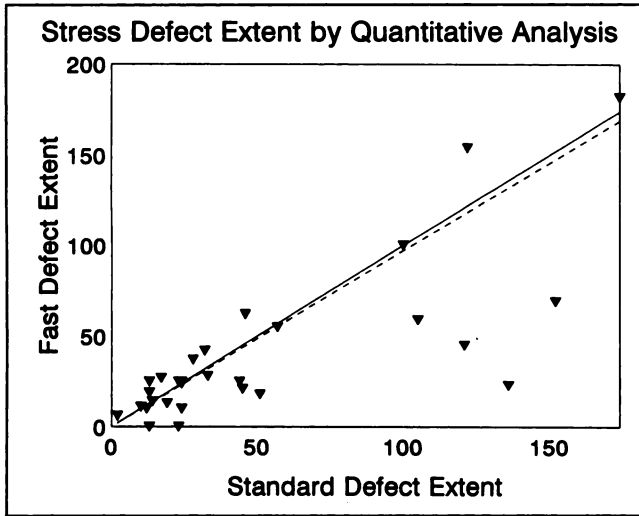
**FIGURE 3.** Comparison of defect extent for 29 stress defects using the standard and fast protocols. Defect extent is automatically determined by comparison of patient data to gender-matched normal limits. Pixels significantly below normal limits (defect counts compared to normal myocardium) are blackened, and the number of such abnormal pixels is quantified as the defect extent.

**Stress Defect Severity by Quantitative Analysis**
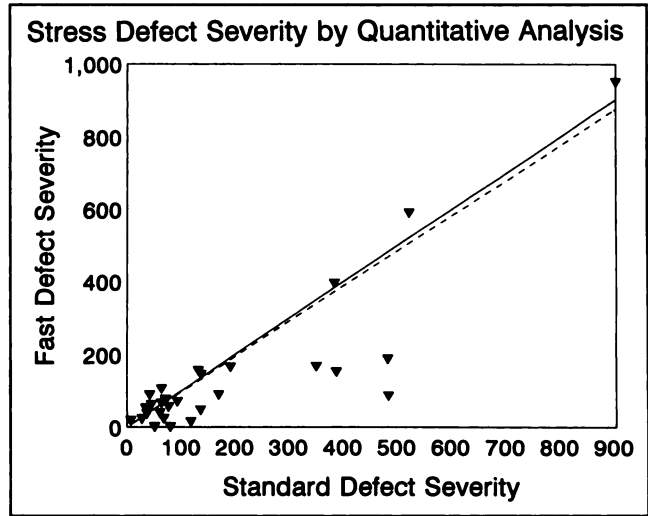
**FIGURE 4.** Comparison of defect severity for 29 stress defects using the standard and fast protocols. Defect severity is also automatically calculated by summing the number of standard deviations below normal limits of each abnormal pixel (see Fig. 3).

was judged to be very good using either method. Both demonstrate slight anterior breast attenuation.

**Patient Two: Inferior Myocardial Infarction**

In this male with a large inferior infarct, the perfusion defect is equally well resolved in the stress images using either the 25-min standard or 8-min fast technique (Fig. 8). Contrast resolution may be slightly greater with the standard technique.

**Patient Three: Multivessel Coronary Disease**

This man had sustained a prior inferior infarct and had multivessel disease, including a 70% stenosis of a small diagonal branch of the left anterior descending coronary

artery (Fig. 9). Although the inferior defect is seen equally well in stress images using either method, a small basal anterolateral defect in the diagonal coronary territory is appreciated only in the 25-min standard study. This is the only patient in our series of 32 stress studies in whom a documented coronary lesion was detected by only the standard technique.

**DISCUSSION**

In an attempt to meet an increasing demand for service with limited instrumentation and personnel resources, laboratories are sometimes tempted to take shortcuts, principally by shortening image acquisition time. Unfortunately, if not carefully validated, such modifications can potentially result in degradation of image quality, poorer spatial
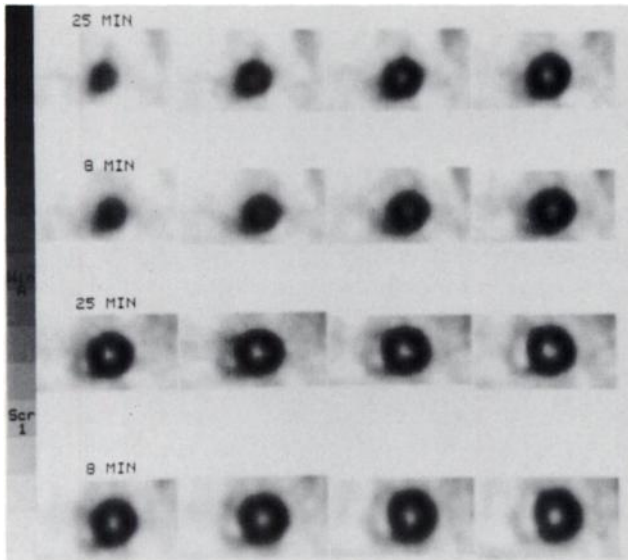
**Rest Defect Extent by Quantitative Analysis**
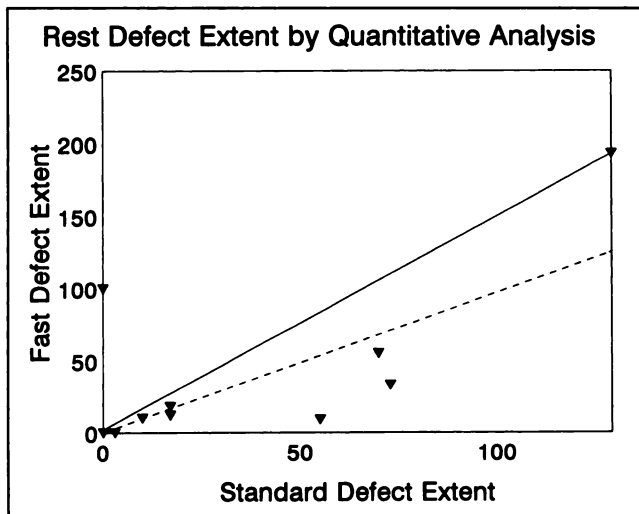
**FIGURE 5.** Comparison of defect extent for eight resting defects using the standard and fast protocols.

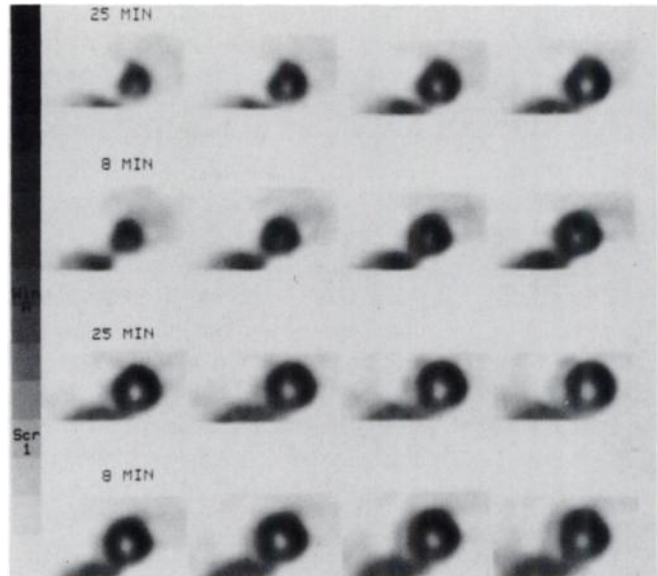**Rest Defect Severity by Quantitative Analysis**
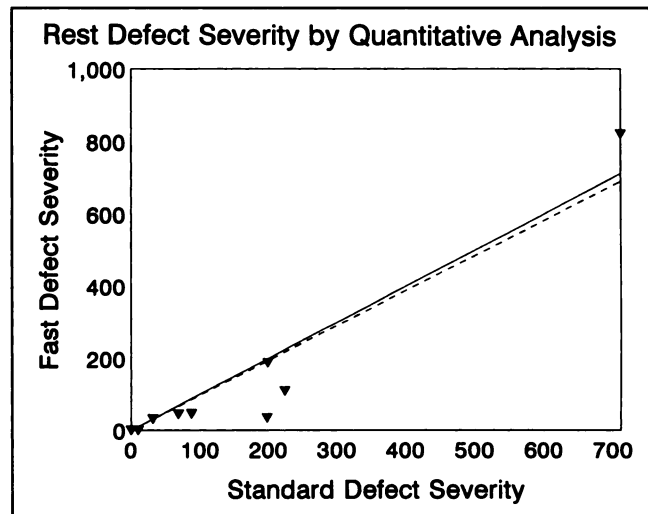
**FIGURE 6.** Comparison of defect severity for eight resting defects using the standard and fast protocols.

**FIGURE 7.** Comparison of standard (25 min) and fast (8 min) stress $^{99m}$Tc-sestamibi SPECT in a normal patient. Short-axis slices are displayed from the apex (upper left) to the base (lower right).

resolution and diagnostic sensitivity, and lower count density and a greater potential for artifacts.

Because of its high count density, $^{99m}$Tc-sestamibi SPECT is somewhat more amenable to such shortcuts than $^{201}$Tl imaging. Taillefer et al. demonstrated that SPECT acquisition time could be halved with no significant decrease in diagnostic accuracy (*4*). In that study, they halved the number of planar projection images within the



**FIGURE 9.** Comparison of standard (25 min) and fast (8 min) stress $^{99m}$Tc-sestamibi SPECT in a patient with a marked inferior perfusion defect due to right coronary artery disease and a small, mild defect in the basal anterolateral wall due to disease of the first diagonal branch of the left anterior descending coronary artery. Short-axis slices are displayed from the apex (upper left) to the base (lower right).



**FIGURE 8.** Comparison of standard (25 min) and fast (8 min) stress $^{99m}$Tc-sestamibi SPECT in a patient with inferior myocardial infarction. Short-axis slices are displayed from near the apex (upper left) to the base (lower right).

180° imaging arc and decreased the time from 20 sec to 15 sec per projection image but did not modify collimation or filtering parameters. Resultant SPECT images were of lower count density than those obtained using standard parameters.

In the present study, we have attempted to partially compensate for the abbreviated acquisition time by selecting a collimator with higher sensitivity and using fewer projections. Also, a lower pass filter was used for processing. Each of these modifications results in higher sensitivity but lower spatial resolution and potentially lower contrast. From our results, which demonstrate that the stress and rest separate-day fast acquisition protocols yield diagnostic results equivalent to longer standard protocols, this trade-off between sensitivity and spatial resolution seems justified.

We did, in fact, subjectively and quantitatively observe a less marked extent and severity of myocardial perfusion defect in a minority of patients. This difference may be due to the factors cited above. Additionally, at least for the stress studies, since fast studies were acquired approximately 20 min after the completion of the standard acquisition protocol in all patients, slight $^{99m}$Tc-sestamibi redistribution may have occurred, rendering defects slightly smaller and less severe (*5*). Thus, although the fast protocol seems to offer a reasonable alternative to the longer, standard protocol, because of the decreased defect extent and severity observed in a minority of patients, it should be used judiciously in patients in whom longer acquisition is impractical. Moreover, the ability to perform gated SPECT and obtain multiple frames per cardiac cycle allowing for assessment of ventricular function has not yet been documented.
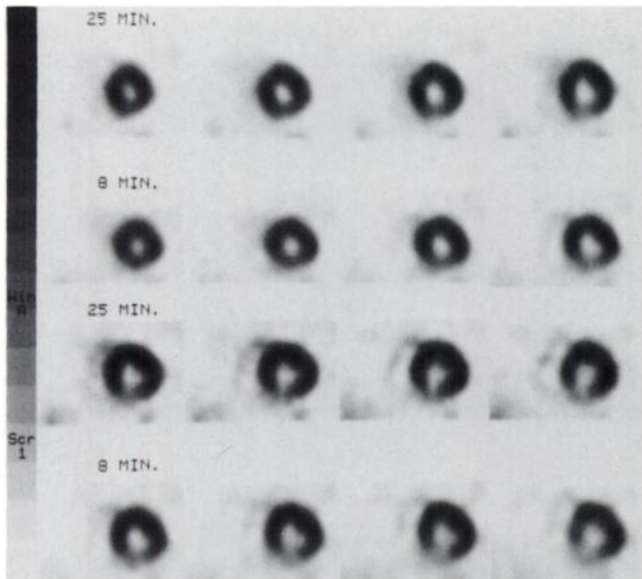
Perhaps the greatest potential advantage of the fast acquisition protocol is improved patient tolerance, particularly for individuals with musculoskeletal disorders and claustrophobia, and consequently less likelihood of patient motion. Motion artifacts are a frequent cause of false-positive myocardial perfusion scans. Less patient motion would decrease the likelihood of such artifacts and potentially improve test specificity.

Another practical advantage of the fast protocols described in this report is improved laboratory efficiency. By decreasing the total image acquisition time for a stress and rest $^{99m}$Tc-sestamibi perfusion time from 50 min to 18 min, more patients can be imaged using the same equipment and personnel resources. For instance, in a laboratory performing six perfusion scans daily using a single camera, total image acquisition time would be reduced from 300 min (5 hr) to 108 min (1 hr, 48 min). This time savings could allow for three additional studies to be performed daily.

The fast acquisition protocols we have described are designed for a single-headed camera. Acquisition time may also be shortened using multiheaded SPECT detector systems, which have been introduced more recently. Moreover, all scans reported in this study were acquired with a step-and-shoot acquisition, using 64 stops for the standard protocols and 32 stops for the fast protocols. Recently continuous acquisition modes have become commercially available (6). With continuous acquisition, the time when the camera is not acquiring between stops is eliminated, thus increasing image count density by approximately 20%. An alternate use of the continuous acquisition mode would be to decrease acquisition time but maintain the same count density. Although this method would not result in as much time savings as the fast protocols we have described, there would be no potential for image degradation from the "shortcuts" we have adopted. Alternately, multidetector imaging and/or the continuous mode acquisition could be combined with the fast protocols we have described to decrease acquisition time even further.

## CONCLUSION

We conclude that the fast stress and rest acquisition protocols we have developed decrease image acquisition times while maintaining adequate counting statistics for clinically useful images. As demonstrated by both visual and quantitative analysis, defect recognition and characterization are nearly the same with these fast protocols as compared to standard methods. The consequent decrease in imaging time results in improved patient tolerance with possibly fewer motion artifacts, and also increased laboratory throughput.

## REFERENCES

1. Garcia EV, Cooke CD, Van Train KF, et al. Technical aspects of myocardial SPECT imaging with technetium-99m-sestamibi. Am J Cardiol 1990;66: 23E-31E.
2. Roy L, Van Train K, Bietendorf J, et al. An optimized protocol for detection of coronary artery disease using technetium-99m sestamibi. J Nucl Med Technol 1991;19:63-67.
3. Van Train KF, Areeda J, Garcia EV, et al. Quantitative same-day rest-stress technetium-99m-sestamibi SPECT: definition and validation of stress normal limits and criteria for abnormality. J Nucl Med 1993;34:1494-1502.
4. Taillefer R, Lambert R, Bisson G, et al. Technetium-99m-sestamibi myocardial SPECT imaging: comparison between a short (8 minutes) and standard (21 minutes) data acquisition time in diagnosis of coronary artery disease [Abstract]. J Nucl Med 1992;33:855.
5. Taillefer R, Primeau M, Costi P, Lambert R, Leveille J, Latour Y. Technetium-99m-sestamibi myocardial perfusion imaging in detection of coronary artery disease: comparison between initial (1 hr) and delayed (3 hr) postexercise images. J Nucl Med 1991;32:1961-1965.
6. Leppo JA, DePuey EG, Johnson LL. A review of cardiac imaging with sestamibi and teboroxime. J Nucl Med 1991;32:2012-2022.